

Lithium insertion behaviour of manganese or molybdenum substituted $\text{Li}_{1+x}\text{V}_3\text{O}_8$

Jin Kawakita*, Hirono Katagiri, Takashi Miura, Tomiya Kishi

Department of Applied Chemistry, Faculty of Science and Technology, Keio University, Hiyoshi 3-14-1, Kohoku-ku, Yokohama 223, Japan

Accepted 14 November 1996

Abstract

Mn(IV) or Mo(VI) substituted single-phase compounds having a nominal composition $\text{Li}_{1+y}\text{Mn}_y\text{V}_{3-y}\text{O}_8$ ($0 < y < 0.1$) and $\text{LiMo}_y\text{V}_{3-y}\text{O}_8$ ($0 < y < 0.3$), respectively, have been obtained by solid-state reaction. Electrochemical measurements revealed different influences of substitution on the lithium insertion behaviours. While substitution of V(V) with Mn(IV) and introduction of Li(I) into the interlayer decrease the insertion limit of lithium, substitution of V(V) with Mo(VI) shows a featureless discharge curve without changing the insertion limit. The ionic sites available for Li^+ occupation between the layers rather than the electronic sites offered by V(V) are considered to determine the insertion limits of lithium into $\text{Li}_{1+x}\text{V}_3\text{O}_8$. © 1997 Elsevier Science S.A.

Keywords: Lithium vanadate oxides; Substitution; Manganese; Molybdenum; Lithium insertion limit

1. Introduction

Vanadium oxides possess excellent properties as cathode materials for lithium secondary batteries, especially such as high charge densities [1–5]. Together with V_2O_5 and V_6O_{13} , $\text{Li}_{1+x}\text{V}_3\text{O}_8$ is also a promising cathode material because of the following characteristics [6–8]: three equivalent lithium accommodated in $\text{Li}_{1+x}\text{V}_3\text{O}_8$ at a high average potential of about 2.6 V, high rate capability connected to a high chemical diffusion coefficient of lithium (\bar{D}_{Li}), and long cycle life due to an outstanding structural stability in lithium insertion and extraction. Among three equivalent Li^+ ions accommodated in $\text{Li}_{1+x}\text{V}_3\text{O}_8$, De Picciotto et al. [9] reported that in a chemical lithium insertion Li^+ ions are reversibly inserted and extracted in a single-phase reaction in the range of $0 < x < 2.0$, whereas for $2.0 < x < 3.0$ the reaction proceeds in the two-phase system. The new phase has a defect rock-salt structure and returns to the parent structure with a slight modification during lithium extraction.

Pistoia et al. [6] reported a similar result for the electrochemical lithium insertion. As electrons injected simultaneously with lithium insertion are localized at the vanadium ions, a high lithium concentration causes a repulsion between

inserted Li^+ ions, and this effect induces the phase transformation. Aimed to delocalize inserted electrons, Pistoia et al. [10] investigated the effects of substitution of V(V) with Mo(VI) and Cr(VI) on the discharge behaviour, and found an unexpected decrease in discharge capacities. Factors controlling the insertion limits and phase transformation are not yet clear, and it will therefore be of interest to investigate the effects of the substitution of V(V) with Mn(IV) or Mo(VI) on the lithium insertion behaviour. For the former, an equivalent amount of Li(I) between layers is necessary to maintain the electrical neutrality. For the latter, substitution causes an equivalent formation of V(IV).

2. Experimental

Mn(IV) or Mo(VI) substituted γ -bronzes, with the formula of $\text{Li}_{1+y}\text{Mn}_y\text{V}_{3-y}\text{O}_8$ or $\text{LiMo}_y\text{V}_{3-y}\text{O}_8$ were prepared, referring to the method described by Pistoia et al. [11], as follows. V_2O_5 obtained by decomposition of NH_4VO_3 (Soekawa Chemicals, >99%) at 500 °C for 24 h and Li_2CO_3 (Yoneyama Chemical Industries, >99.0%) with the appropriate amounts of MnO_2 (EMD, Daiichi) or MoO_3 (Soekawa Chemicals, >99.9%) were mixed in an agate mortar. The mixture was pressed into a pellet and heated at 680 °C for

* Corresponding author

24 h and then cooled slowly down to room temperature in three steps (cooled at a rate of 13.3 °C/h to 520 °C and held at this temperature for 12 h and further cooled down to room temperature at a rate of 7.2 °C/h). $\text{Li}_{1.2}\text{V}_3\text{O}_8$ was also prepared by the same method as a reference material. The composition of each sample was determined by atomic absorption analysis (Hitachi, 180-50 AAS) of each metal element. X-ray diffraction (XRD, Rigaku, RINT-1300, Cu $K\alpha$ radiation with nickel filter) and infrared spectroscopic (IR) methods (Bio-Rad, FTS-65, KBr disk method) were used for structural analysis. X-ray photoelectron spectroscopy (XPS) was carried out for determination of the valence of manganese in Mn-substituted oxides.

A mixture of the sample powder (sieved under 38 μm), acetylene black (Denka black, Denkikagaku Kogyo) and poly(tetrafluoroethylene) in a weight ratio of 80:15:5 was pressed into a pellet form onto a porous nickel sheet, which was connected to a lead wire by silver paste. The counter side of the pellet was used as the electrodes (surface area of 0.196 cm^2), and the rest part of the pellet surface and a lead wire were coated by a silicone resin. All electrochemical measurements were performed using a cylindrical glass cell. Lithium wires (Aldrich, >99.9%, diameter: 3.2 mm) were used as the counter and the reference electrodes. 1 M LiClO_4/PC solution (Mitsubishi Chemical, containing $\text{H}_2\text{O} < 20$ ppm) was used as the electrolyte. Galvanostatic discharge was performed in the current density of 0.25 or 0.1 mA cm^{-2} with a

potentiostat (Toho Technical Research, 2092 and PS-08). Cyclic voltammetry was performed at a scanning rate of 0.01 mV s^{-1} with a potentiostat described above and a function generator (Hokuto Denko, HB-104).

3. Results and discussion

3.1. Single phase region of $\text{Li}_{1+y}\text{Mn}_y\text{V}_{3-y}\text{O}_8$ and $\text{LiMo}_y\text{V}_{3-y}\text{O}_8$

Examples of X-ray diffraction (XRD) patterns of $\text{Li}_{1+y}\text{Mn}_y\text{V}_{3-y}\text{O}_8$ were shown in Fig. 1(a)–(c). Almost the same patterns were obtained with the samples of $0 < y < 0.1$, and beyond this composition the additional lines attributed to LiVO_3 (marked with arrows) appeared. The latter phenomenon would be related to the addition of excess lithium with the ratio of $\text{Li}/\text{Mn(IV)} + \text{V(V)} = 1 + y/3$ to balance the cationic valences, as the addition of lithium to $\text{Li}_{1+y}\text{V}_3\text{O}_8$ in excess caused a formation of LiVO_3 , expected from the phase diagram of $\text{Li}_2\text{O}-\text{V}_2\text{O}_5$ system [12]. XPS data of $\text{Li}_{1+y}\text{Mn}_y\text{V}_{3-y}\text{O}_8$ indicated that manganese existed in the oxides as Mn(IV). The lattice parameters calculated from XRD data were shown in Fig. 2, in which a_0 , (equal to the interlayer distance d_{100} over $\sin \beta$) increased as y increased compared with other parameters at $0 < y < 0.1$. In the case of $\text{Li}_{1+y}\text{V}_3\text{O}_8$ the interlayer distance tended to increase as x increased by comparing at $x=0$ and $x=1.6$ [7], where the Li^+ ions occupied the tetrahedral sites and an equivalent amount of V(V) changed to V(IV). Li(I) content in the interlayer space is predominant to control the interlayer distances, and almost the same situation held for the case of $\text{Li}_{1+y}\text{Mn}_y\text{V}_{3-y}\text{O}_8$.

From the same analysis for $\text{LiMo}_y\text{V}_{3-y}\text{O}_8$ (see Fig. 1(a),(d),(e)), almost the same patterns were obtained with the samples $0 < y < 0.3$, and at $y > 0.3$ the additional

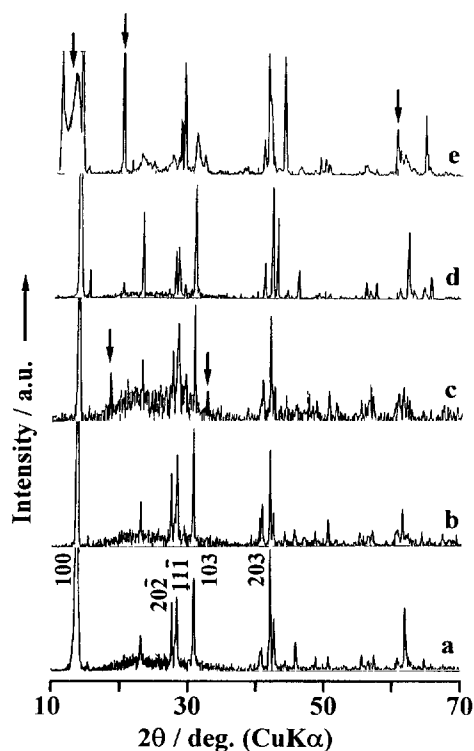


Fig. 1 Powder X-ray diffraction patterns of Mn- and Mo-substituted compounds: (a) $\text{Li}_{1.2}\text{V}_3\text{O}_8$; (b) $\text{Li}_{1.1}\text{Mn}_{0.1}\text{V}_{2.9}\text{O}_8$; (c) $\text{Li}_{1.2}\text{Mn}_{0.2}\text{V}_{2.8}\text{O}_8$; (d) $\text{LiMo}_{0.2}\text{V}_{2.8}\text{O}_8$, and (e) $\text{LiMo}_{0.5}\text{V}_{2.5}\text{O}_8$.

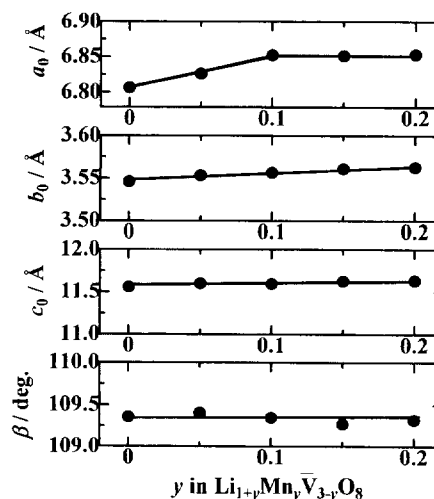


Fig. 2 Lattice parameters of $\text{Li}_{1+y}\text{Mn}_y\text{V}_{3-y}\text{O}_8$.

diffraction lines attributed to V_2O_5 (marked with arrows) were observed. The lattice parameters calculated from XRD data (see Fig. 3), in which a_0 , c_0 and β decreased linearly at $0 < y < 0.3$ and were almost constant at $y > 0.3$. These results indicated that a limit of the primary single-phase region existed at about $y = 0.3$. In IR spectra the absorption bands ascribed to the stretching vibration of Mo–O in MoO_3 (marked with arrows) were clearly observed at $y = 0.5$, as shown in Fig. 4, and this fact with XRD data indicated that beyond the single-phase region V_2O_5 and MoO_3 (both presumably partly lithiated) appeared as the second phases. Sub-

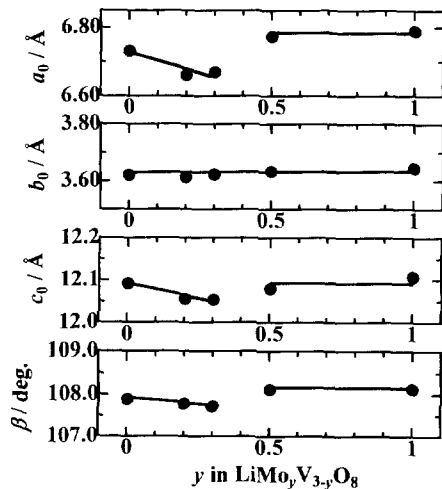


Fig. 3. Lattice parameters of $LiMo_yV_{3-y}O_8$.

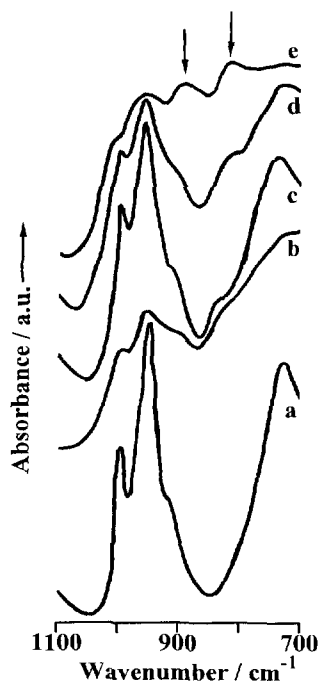


Fig. 4. IR spectra of $LiMo_yV_{3-y}O_8$: (a) $y = 0.0$; (b) $y = 0.2$; (c) $y = 0.3$; (d) $y = 0.5$, and (e) $y = 1.0$.

stitution of V(V) with Mo(VI) and formation of an equivalent amount of V(IV) without adding Li(I) in the interlayer space caused a decrease in the interlayer distance, and substitution of V(V) with Mo(VI) predominates to control the interlayer distance, and this effect is larger than in the case of substitution with Mn(IV).

3.2. Lithium insertion of $Li_{1+y}Mn_yV_{3-y}O_8$ and $LiMo_yV_{3-y}O_8$

Examples of the galvanostatic discharge curves of $Li_{1+y}Mn_yV_{3-y}O_8$ were shown in Fig. 5, in which the abscissa was designated by x in $Li_{1+y+x}Mn_yV_{3-y}O_8$ calculated from the amounts of a passed electricity. The limit of lithium insertion (up to 1.5 V versus Li^+/Li) decreased with increasing y values. In order to compare the length of the

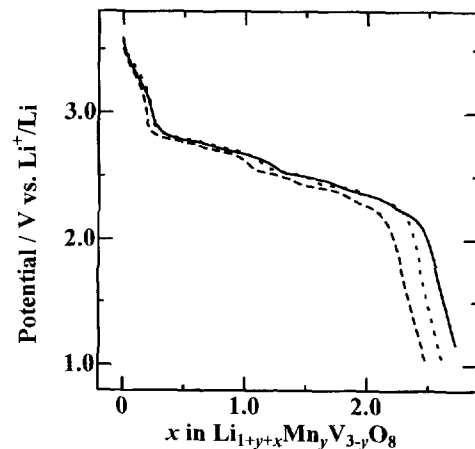


Fig. 5. Discharge curves of $Li_{1+y}Mn_yV_{3-y}O_8$ at -0.25 mA cm^{-2} : (—) $y = 0.00$; (· · ·) $y = 0.05$, and (---) $y = 0.10$.

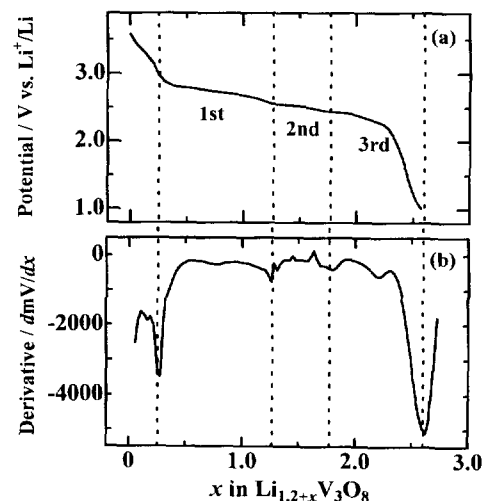


Fig. 6. (a) Discharge and (b) its derivative curves for $Li_{1.2-x}V_3O_8$ at -0.25 mA cm^{-2} .

plateaus found in the discharge curves, the derivative dE/dx was calculated and shown in Fig. 6(b), together with discharge curve (Fig. 6(a)). From those figures three plateaus found in $\text{Li}_{1+y}\text{V}_3\text{O}_8$ were observed clearly (in contrast to the case of Mo-substituted oxides). The insertion limit of each plateau changed with y as shown in Fig. 7. According to De Picciotto's proposal [9], the first and second plateaus correspond to lithium insertion into two kinds of tetrahedral sites with different stabilization energy for the inserted Li^+ ions, and it was found that both the plateaus shortened as y increased. This suggested that the possible numbers of occupation decrease in both sites as substitution of V(V) with Mn(IV) and also the preexistence of the Li^+ ions proceed. The third plateau started at smaller x values and the third plateau region (x values) increased as y increased. Total amount of insertion decreased as y increased.

These effects of the substitution on the insertion indicate that the single-phase insertion limit and the lithium content of the final products (up to 1.5 V) decreased by the substitution, and this decrement is larger than that estimated from amount of V(V), i.e. $3 - y$. This suggests that the sites available for the Li^+ ions decrease by substitution of V(V) with Mn(IV) through instabilization of the sites occupied by the Li^+ ions.

The cyclic voltammograms shown in Fig. 8, were the same shape but a little more asymmetric than that obtained by Pistoia et al. [8] for $\text{Li}_{1+y}\text{V}_3\text{O}_8$, owing to kinetic factors. Insertion processes for $\text{Li}_{1.1}\text{Mn}_{0.1}\text{V}_{2.9}\text{O}_8$ proceeded through the same steps as $\text{Li}_{1+y}\text{V}_3\text{O}_8$ and showed that the cathodic third peak had a reversible nature compared to the other peaks as in the case of $\text{Li}_{1+y}\text{V}_3\text{O}_8$.

Examples of the galvanostatic discharge curves for Li-Mo- V_{3-y}O_8 were shown in Fig. 9. The limits of insertion were about $x = 3.0$, almost independent of y , and the plateaus found in the discharge curve for $\text{Li}_{1+y}\text{V}_3\text{O}_8$ became featureless as y increased. The latter phenomenon would be caused by a distribution of the site stabilization energy for the inserted Li^+ ions by a random substitution of vanadium with

molybdenum, and similar results were observed for $\text{Mo}_y\text{V}_{2-y}\text{O}_5$ [13,14]. As substitution of V(V) with Mo(VI) causes a change of the equivalent amounts of V(V) to V(IV) and the formal valences of the cations in the oxides are expressed as $\text{Li}(\text{I})\text{Mo}(\text{VI})_y\text{V}(\text{IV})_{3-y}\text{O}_8$. If V(V) is only an electron accepting component the insertion limit is expected to be $3 - 2y$, and if Mo(VI) takes part in the reduction, it will become $3 - y$. For the almost constant insertion limit of $x = 3.0$ independent of y , a possible explanation will be that the lithium insertion limit is controlled by an ionic site limitation, and the electronic sites provided by V(V) and Mo(VI) or V(IV) do not restrict lithium insertion. For the sample with $y = 0.5$, which included MoO_3 phase, the discharge curve had a small hump at the end of the profile, and this could be attributed to the reduction of Mo(VI) to Mo(V). In contrast, any additional step in the discharge curve was not be found for the primary single-phase samples.

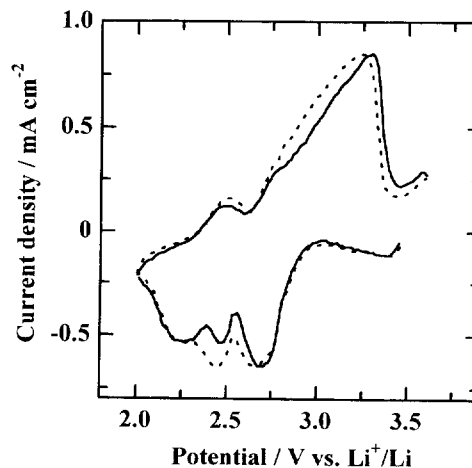


Fig. 8. Cyclic voltammogram at 0.01 mV s^{-1} : (—) $\text{Li}_{1.1}\text{Mn}_{0.1}\text{V}_{2.9}\text{O}_8$, and (---) $\text{Li}_{1.2}\text{V}_3\text{O}_8$.

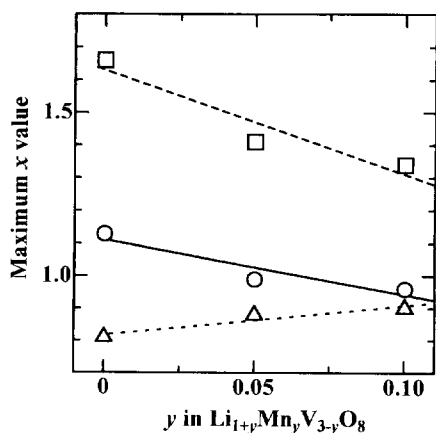


Fig. 7. Maximum x value at each plateau of $\text{Li}_{1+y}\text{Mn}_y\text{V}_{3-y}\text{O}_8$: (○) first step, (□) first + second steps, and (△) third step

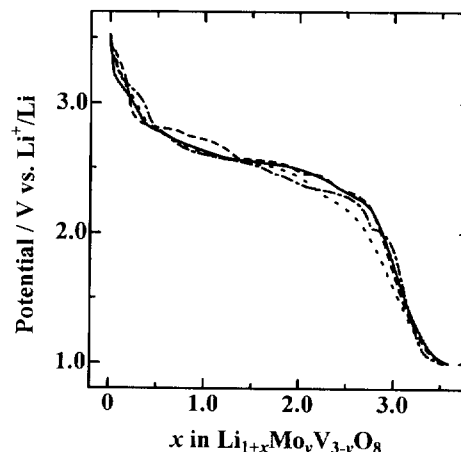


Fig. 9. Discharge curves of $\text{LiMo}_y\text{V}_{3-y}\text{O}_8$ at -0.1 mA cm^{-2} : (---) $y = 0.0$; (—) $y = 0.2$, (···) $y = 0.3$, and (- · -) $y = 0.5$

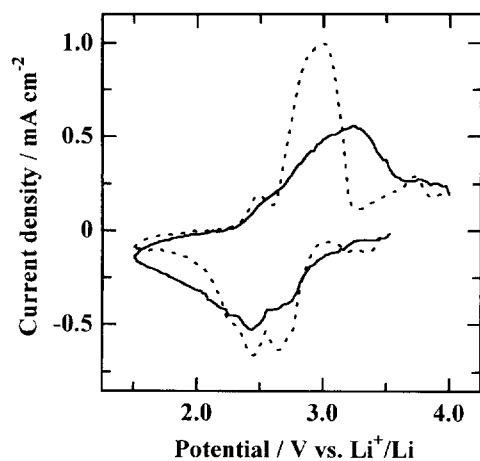


Fig. 10. Cyclic voltammogram at 0.01 mV s^{-1} (—) $\text{LiMo}_{0.2}\text{V}_{2.8}\text{O}_8$ and (---) $\text{Li}_{1.2}\text{V}_3\text{O}_8$.

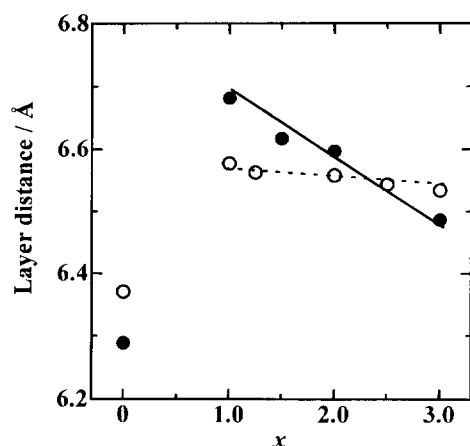


Fig. 11. Layer distance d_{100} : (○) $\text{Li}_{1.2+x}\text{V}_3\text{O}_8$, and (●) $\text{Li}_{1+x}\text{Mo}_{0.2}\text{V}_{2.8}\text{O}_8$.

In the cyclic voltammogram shown in Fig. 10 a clear extra cathodic peak ascribed to the reduction of Mo(VI) or V(IV) could not be found for $\text{LiMo}_{0.2}\text{V}_{2.8}\text{O}_8$. Interlayer distance changed with x almost independent of y , as shown in Fig. 11. As shown in Fig. 12, any new diffraction lines were not found, compared with the case of the chemical lithium insertion [9], where several lines attributed to the defect rock-salt structure were observed. In some cases of electrochemical lithium insertion the additional diffraction lines at about 14° in 2θ were observed [8], but this line was not observed in this case. From these facts, the phase transition to a defect rock-salt structure [9] did not occur at $2.0 < x < 3.0$, as shown in Fig. 12.

4. Conclusions

Mn(IV) and Mo(VI) substituted $\text{Li}_{1+y}\text{Mn}_y\text{V}_{3-y}\text{O}_8$ and $\text{LiMo}_y\text{V}_{3-y}\text{O}_8$ had single-phase regions at $0 < y < 0.1$ and $0 < y < 0.3$, respectively.

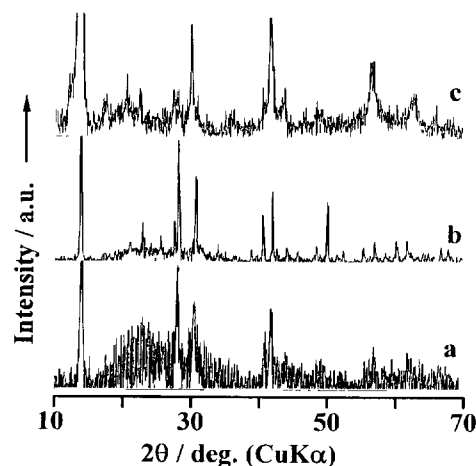


Fig. 12. Powder XRD patterns of the lithiated samples after discharge to 1.5 V: (a) $\text{Li}_{1.2}\text{V}_3\text{O}_8$, (b) $\text{Li}_{1.1}\text{Mn}_{0.1}\text{V}_{2.9}\text{O}_8$, and (c) $\text{LiMo}_{0.2}\text{V}_{2.8}\text{O}_8$.

Electrochemical measurements revealed that substitution affected the insertion behaviours in a different manner. Simultaneous introduction of substituted Mn(IV) and Li(I) in the interlayer decreases the insertion limit of lithium, and substitution of V(V) with Mo(VI) with a formation of an equivalent amount of V(IV) gives a featureless discharge curves without changing the insertion limit. The limit of lithium insertion seems to be controlled rather by available ionic sites for lithium occupation than electronic sites offered by V(V) and Mo(VI).

Acknowledgements

The authors thank to Kato Kagaku Shinkokai for financial support and wish to thank to Mitsubishi Chemical for kindly providing the electrolyte.

References

- [1] D.W. Murphy, P.A. Christian, F.J. DiSalvo and J.N. Carides, *J. Electrochem. Soc.*, **126** (1979) 497.
- [2] K.M. Abraham, J.L. Goldman and M.D. Dempsey, *J. Electrochem. Soc.*, **128** (1981) 2493.
- [3] N. Kumagai, K. Tanno, T. Nakajima and N. Watanabe, *Electrochim. Acta*, **28** (1983) 17.
- [4] Y. Muranushi, T. Mura, T. Kishi and T. Nagai, *Denki Kagaku*, **54** (1986) 691.
- [5] N. Koshiba, K. Takada, M. Nakanishi and Z. Takehara, *Denki Kagaku*, **62** (1994) 332.
- [6] S. Panero, M. Pasquali and G. Pistoia, *J. Electrochem. Soc.*, **130** (1983) 1225.
- [7] G. Pistoia, S. Panero, M. Tocci, R.V. Moshtev and V. Manev, *Solid State Ionics*, **13** (1984) 311.
- [8] G. Pistoia, M. Pasquali, M. Tocci, R.V. Moshtev and V. Manev, *J. Electrochem. Soc.*, **132** (1985) 281.

- [9] L.A. de Picciotto, K.T. Adendorff, D.C. Liles and M.M. Thackeray, *Solid State Ionics*, 62 (1993) 297.
- [10] M. Pasquali, G. Pistoia, V. Manev and R.V. Moshtev, *J. Electrochem. Soc.*, 133 (1986) 2454.
- [11] G. Pistoia, M. Pasquali, M. Tocci, V. Manev and R.V. Moshtev, *J. Power Sources*, 15 (1985) 13.
- [12] D.G. Wickham, *J. Inorg. Chem.*, 27 (1965) 1939.
- [13] Y. Muranushi, T. Miura, T. Kishi and T. Nagai, *J. Power Sources*, 20 (1987) 187.
- [14] K. West, B. Zachau-Christiansen, S. Skaarup and T. Jacobsen, *Solid State Ionics*, 53–56 (1992) 356.